Am J Physiol Heart Circ Physiol 293: H448–H456, 2007.
First published March 16, 2007; doi:10.1152/ajpheart.00035.2007.

Myocardial hypoxia-inducible HIF-1α, VEGF, and GLUT1 gene expression is associated with microvascular and ICAM-1 heterogeneity during endotoxemia

Ryon M. Bateman, Chiho Tokunaga, Thoma Kareco, Delbert R. Dorscheid, and Keith R. Walley

University of British Columbia Critical Care Research Laboratories, Department of Medicine, St. Paul's Hospital, Vancouver, British Columbia, Canada

Submitted 16 March 2007; accepted in final form 19 March 2007

Bateman RM, Tokunaga C, Kareco T, Dorscheid DR, Walley KR. Myocardial hypoxia-inducible HIF-1α, VEGF, and GLUT1 gene expression is associated with microvascular and ICAM-1 heterogeneity during endotoxemia. *Am J Physiol Heart Circ Physiol* 293: H448–H456, 2007. First published March 16, 2007; doi:10.1152/ajpheart.00035.2007.—The systemic inflammatory response to infection is the leading cause of mortality in North American intensive-care units. Although much is known about inflammatory mediators, the relationships between microregional inflammation, microvascular heterogeneity, hypoxia, hypoxia-inducible gene expression, and myocardial dysfunction are unknown. Male Sprague-Dawley rats were injected intraperitoneally with LPS to test the hypothesis that sepsis-induced local inflammation and increased microvascular heterogeneity are spatially and temporally associated with hypoxia, hypoxia-inducible gene expression, and decreased left-ventricular contractility. Using a combination of three-dimensional microvascular imaging, tissue Po_2, and pressure-volume conductance measurements, we found that 5 h after LPS, minimum oxygen-diffusion distances increased ($P < 0.05$), whereas tissue oxygenation and contractility both decreased ($P < 0.05$) in the left ventricle. Real-time RT-PCR analysis revealed that the hypoxia-inducible genes hypoxia-inducible factor (HIF)-1α, VEGF, and glucose transporter (GLUT) 1 were all upregulated ($P < 0.05$) in the left ventricle. Tissue regions expressing ICAM-1, obtained by using laser-capture microdissection, had increased HIF-1α and GLUT1 ($P < 0.05$) gene expression. VEGF gene expression was more diffuse. In LPS rats, GLUT1 gene expression correlated ($P < 0.05$) with left-ventricular contractility. In 5-h hypoxic cardiomyocytes, we found strong transient HIF-1α, weak VEGF, and greater prolonged GLUT1 gene expression. By comparison, the HIF-1α-GLUT1 gene-induction pattern was reversed in the left ventricle of LPS rats. Together, these results show that LPS induces hypoxia in the left ventricle associated with increased microvascular heterogeneity and decreased contractility. HIF-1α and GLUT1 gene induction are related to a heterogeneous ICAM-1 expression and may be cardioprotective during the onset of septic injury.

sepsis; microcirculation; inflammation; heart

SEPSIS, THE SYSTEMIC INFLAMMATORY response to infection, is the leading cause of death in North American intensive-care units. As many patients die annually from sepsis-related cardiovascular collapse or multiple organ failure as do from acute myocardial infarction (1). Inadequate oxygen supply is probably the most important pathophysiological mechanism leading to myocardial dysfunction (25) and may play an important role in sepsis pathophysiology and decreased heart function, because progressive hypoxia reduces left ventricle contractility (42). Although direct evidence of tissue hypoxia within the septic heart has been lacking (4, 22, 23), evidence of diminished blood flow autoregulation (5) and loss of myocardial capillary density (6) suggest that a maldistribution of capillary blood flow (17) exists within the septic heart and that microvascular oxygen transport (8) has been compromised. As a consequence of sepsis-induced microvascular dysfunction, oxygen supply may be inadequate at the microregional level to support normal heart metabolism and function.

Although initial cytoprotective mechanisms to hypoxia involve protein modifications, a prolonged adaptive response to hypoxia requires change in gene expression (25). The master regulator of oxygen homeostasis is the nuclear transcription factor hypoxia-inducible factor-1 (HIF-1) (37, 43). HIF-1 is composed of a constitutively expressed β-subunit (HIF-1β) and an oxygen-dependent α-subunit (HIF-1α) (25, 36). The HIF-1 system regulates over 70 genes containing hypoxia-response elements in their promoter regions, including glucose transporter (GLUT) 1 and VEGF (46). HIF-1 activity is regulated by expression of the HIF-1α subunit, which is controlled by the balance between its synthesis, which is modulated by inflammatory mediators (10, 18), and its degradation, which is modulated by oxygen-dependent ubiquitination and proteasomal degradation under normoxic conditions (36, 39, 47).

During the onset of sepsis, the complex relationships between microregional inflammation, microvascular heterogeneity, hypoxia, hypoxia-inducible gene expression, and organ function are not well understood in general nor in the heart specifically. We hypothesize that sepsis induces local inflammation and increased microvascular heterogeneity, which is spatially and temporally associated with hypoxia and hypoxia-inducible gene expression, which in turn modulates heart function. To address this hypothesis, we studied the left ventricle of rats injected with LPS compared with controls. First, we imaged the myocardial microvasculature in three dimensions by using laser-scanning confocal microscopy. On the basis of these images, we determined whether LPS altered microvascular oxygen transport by increasing oxygen-diffusion distances in the left ventricle. Second, we directly measured changes in myocardial tissue oxygenation by using a fiber optic Po_2 probe. Third, we determined whether this degree of myocardial hypoxia could stabilize the HIF-1α subunit and trigger hypoxia-inducible gene expression of HIF-1α, VEGF, and GLUT1 in isolated cardiomyocytes and the left ventricle. Fourth, by assessing microregional hypoxia-inducible gene expression in tissue expressing ICAM-1, we were able to characterize gene expression as either homogeneous or heterogeneous relative to a local marker of tissue inflamma-

Address for reprint requests and other correspondence: K. R. Walley, St. Paul's Hospital, 1081 Burrard St., Vancouver, BC V6Z 1Y6, Canada (e-mail: kwalley@mrl.ubc.ca).

The costs of publication of this article were defrayed in part by the payment of page charges. The article must therefore be hereby marked "*advertisement*" in accordance with 18 U.S.C. Section 1734 solely to indicate this fact.

tion. Finally, we examined the relationship between hypoxia-inducible gene expression and decreased heart contractility, a clinically important sepsis event.

MATERIALS AND METHODS

Animal model of endotoxemia. Nonfasting male Sprague-Dawley rats (250–300 g) were anesthetized with 3% isoflurane, injected intraperitoneally with LPS (10 mg/kg, *Escherichia coli* serotype 0111:B4; Sigma, St. Louis, MO), and allowed to recover. Five hours after LPS administration, animals were reanesthetized and placed on a heating pad to maintain internal core temperature between 36 and 37°C. This normotensive model was used to investigate the acute effects of the systemic inflammatory response to LPS on myocardial function, microvascular and ICAM-1 heterogeneity, tissue oxygenation, and hypoxia-inducible gene expression. White blood cell and platelet counts were assessed as markers of systemic inflammation, and ICAM-1 expression was used as a marker of local tissue inflammation. Global oxygen transport parameters, hematocrit, and hemoglobin were determined from venous blood (CELL-DYN 3700; Abbott Laboratories, Abbott Park, IL), and arterial oxygen saturation was measured by using pedal-pulse oximetry (Nonin Medical, Plymouth, MN). All investigations conformed with the *Guide for the Care and Use of Laboratory Animals* published by the U.S. National Institutes of Health (NIH publication no. 85–23, revised 1996), and all experimental protocols were approved by the University of British Columbia Animal Care Committee.

Heart function and left ventricular contractility. Five hours after LPS administration, a pressure-volume micromanometer conductance catheter (Millar Mikro-Tip 2.0; Millar Instruments, Houston, TX) was advanced into the left ventricle via the right carotid artery of the anesthetized rat. Measurements of left-ventricular pressure and volume were acquired at steady state and during compression of the inferior vena cava. Data were recorded by using the ARIA P-V conductance system (Millar Instruments). Maximum elastance (E_{max}), a measure of heart contractility relatively independent of cardiac preload and afterload (38), and measures of ventricular pressures and volumes, heart rate, and cardiac output were determined by using PVAN v. 2.9 data-analysis software (Millar Instruments). The P-V catheter was calibrated against known blood volumes according to manufacturer instructions. Following catheter measurement, the heart was excised and 30 mg of left ventricle tissue was harvested in RNA lysis buffer (Qiagen, Mississauga, ON, Canada) and stored at −80°C for target gene-expression analysis (HIF-1α, VEGF, GLUT1) and correlation with heart function (E_{max}).

Myocardial microvascular geometry. Change in myocardial microvascular geometry, a determining factor of microvascular heterogeneity and tissue hypoxia (20, 21), was determined by measuring the minimum oxygen-diffusion distance between tissue and the nearest capillary segment. In a separate experiment, heparin was administered (4000 U/kg ip) to the anesthetized animal 5 h after LPS injection, and the heart was removed and mounted on a Langendorff perfusion system. Circulating blood cells and fibrinogen were washed out by infusion of Krebs solution for 3–5 min. Once the draining solution ran clear, the heart was fixed, and microvascular endothelial membranes were labeled under constant 75-cmH_2O pressure by infusion of 2% paraformaldehyde containing 0.8 mg/40 ml of the fluorescent probe $DiOC_{18}$ (Molecular Probes, Eugene, OR).

A sample of mid-left-ventricle tissue was excised by using a vibratome (Leica VT1000S) and was optically sectioned at 1-μm intervals (60 × 512 × 512 pixels) by using laser-scanning confocal microscopy (×40 dry/0.6 numerical aperture objective; Bio-Rad Radiance Plus). The resulting image stack was deconvolved by using a theoretical point-spread function (XCOSM v. 2.5; Washington University, St. Louis, MO; http://www.ibc.wustl.edu/xcosm). With the use of three-dimensional reconstructions of microvascular networks, minimum oxygen-diffusion distances were calculated on the basis of shortest tissue element voxel-to-capillary distance, as previously described (12). Because distributions were skewed, we calculated the median, 75th percentile, and fraction of myocardium with minimum oxygen-diffusion distances >7 μm, because myocardium farthest from the nearest capillary would be at a relatively higher risk of hypoxia.

Myocardial tissue oxygenation. To determine whether LPS induced myocardial hypoxia by 5 h, a third group of animals was used. In this experiment, the chest of mechanically ventilated animals (Harvard small animal ventilator; Harvard Apparatus, Holliston, MA) was opened by left-sided thracotomy, and a 230-μm-diameter-tip fluorescent-tissue P_{O_2} probe (OxyLite; Oxford Optronics, Oxford, UK) was inserted into the left-ventricular myocardium to a depth of 1–2 mm, which limited tissue damage. A 20-gauge needle was used to guide the probe into the heart muscle and was withdrawn before recording. During the procedure, heart rate and oxygen saturation were monitored. Six 20-s measurements were obtained as quickly as possible and were averaged over the time interval (13). The probe was precalibrated by the manufacturer and was only used if readings were ±10% of true P_{O_2} at 0 and 21% oxygen.

In vitro kinetics of cardiomyocyte expression of hypoxia-inducible genes. Having found that LPS reduced myocardial tissue P_{O_2} to 5 mmHg, we simulated this effect in cardiomyocytes to elaborate the kinetics of HIF-1α protein stabilization and gene expression of the target genes HIF-1α, VEGF, and GLUT1. Cardiomyocytes (65,000/ml) were isolated from healthy animals, as previously described (15), and were placed in a hypoxic chamber (37°C, 5% CO_2 with a P_{O_2} = 5 mmHg, balance N_2). Cells were washed, and the MEM medium was exchanged with medium equilibrated to chamber conditions. Because LPS increases the TNF-α level in plasma (6) and triggers the expression of TNF-α in cardiomyocytes (31), and because TNF-α is also associated with decreased cardiomyocyte contractility (15), we assessed whether TNF-α (50 ng/ml) could also upregulate hypoxia-inducible gene expression under normoxic conditions. Additionally, because we found that LPS induced myocardial hypoxia, cardiomyocytes were treated with TNF-α under hypoxic conditions (a situation that may exist in the septic myocardium) to assess whether a synergistic effect existed between hypoxia and TNF-α stimulation with respect to hypoxia-inducible gene expression. Cells were harvested at 0, 1, 2, 3.5, and 5 h in RLT lysis buffer (Qiagen) and were stored at −80°C for later quantitative real-time RT-PCR measurement of mRNA expression.

In vivo myocardial expression of hypoxia-inducible genes during controlled hypoxia. A separate group of animals was used as a positive in vivo myocardial ischemia control. In this case, mechanically ventilated animals (Harvard small animal ventilator) were subjected to left anterior descending (LAD) coronary artery ligation. After 5 h, hearts were excised and 30 mg of left ventricle was harvested in RLT lysis buffer and stored at −80°C for later quantitative real-time RT-PCR measurement of mRNA expression.

Microregional relationship between ICAM-1 and hypoxia-inducible gene expression. Because LPS stimulates expression of myocardial ICAM-1, a marker of local tissue inflammation, we sought to evaluate the spatial relationship between local inflammation and hypoxia-inducible gene expression. In an additional experiment, 5 h after LPS administration, hearts were removed, covered with optimal cutting temperature compound embedding medium (RA Lamb), and flash frozen in isopentane. The heart was then cut into alternating 8-μm-thick left ventricle sections for immunohistochemical identification of ICAM-1 regions and corresponding tissue sampling using laser capture microdissection.

To identify ICAM-1 regions for laser-capture microdissection, even-numbered sections were fixed in acetone (10 min), blocked with Universal Block (15 min; DAKO, Fort Collins, CO), and incubated with mouse anti-rat ICAM-1 antibody [2 h at room temperature at 1/400 in Tris-buffered saline (TBS-1%) BSA; PharMingen, San Diego, CA]. Washed sections (TBS, pH 7.6) were incubated with

fluorescently labeled secondary rabbit anti-mouse antibody (30 min at 1/20 in TBS-1% BSA; DAKO) and were examined by fluorescent microscopy. To sample myocardial tissue from overexpressed ICAM-1 areas, corresponding odd-numbered tissue sections were treated with 75% ethanol (30 s), transferred to diethyl pyrocarbonate water (5 s), stained with 100 μl HistoGene staining kit (Arcturus Biosciences, Mountain View, CA), and placed in diethyl pyrocarbonate water (5 s). Water was removed by successive treatments in 75, 95, and 100% ethanol (30, 30, and 300 s, respectively), and the ethanol was removed by xylene (5 min). Regions of ICAM-1 myocardial tissue were sampled by using an Arcturus PixCell II laser-capture microdissection system (Arcturus Bioscience) operating at 50-mW laser power with a laser spot of 7.5 μm and 450-μs duration. Tissue samples were harvested in RLT lysis buffer and were stored at −80°C for later quantitative real-time RT-PCR measurement of mRNA expression.

Quantitative real-time RT-PCR. Two micrograms of RNA, isolated by using a mini-column (Qiagen), was assayed by using QuantiTect SYBR Green one-step RT-PCR (Qiagen). Quantitative real-time RT-PCR was performed by using an ABI 7900 (Applied Biosystems, Foster City, CA) with the sense and antisense primers listed in Table 1. All target genes were evaluated simultaneously under the same reaction conditions: 50°C for 30 min, 9°C for 15 min, and then 40 cycles of 94°C for 15 s, 60°C for 30 s, and 72°C for 30 s. Samples were analyzed by quantification software (SDS 2.1; Applied Biosystems). Products were confirmed by electrophoresis on a 3% agarose gel stained with ethidium bromide. For each treatment group, HIF-1α, VEGF, and GLUT1 gene expressions were first normalized to 18s ribosomal mRNA. To assess differences between groups, the normalized gene-expression data were then expressed relative to the corresponding normalized control gene-expression data (i.e., gene induction is the ratio of treatment to control gene expression) and were compared on the basis of differences in gene induction.

HIF-1α protein expression. HIF-1α protein from isolated cardiomyocytes was quantified by using Western blot. Briefly, cardiomyocytes were harvested in lysis buffer (in mM: 20 Tris·HCl, pH 7.5, 150 NaCl, 1 EDTA, 1 EGTA, 2.5 pyrophosphate, and 1 Na_3VO_4) containing a protease inhibitor cocktail (Roche Diagnostics, Mannheim, Germany). Twenty micrograms of protein was loaded on a 7.5% SDS-PAGE gel, electrophoresed (80 V for 30 min followed by 110 V for 90 min), transferred to nitrocellulose membrane (20 V for 16 h), blocked with 5% nonfat milk in TBS-Tween 20 for 1 h at room temperature, and incubated with anti HIF-1α primary antibody (Novus Biologicals, Littleton, CO) in TBS-Tween 20 (5% BSA) at 4°C overnight. The membrane was incubated with horseradish peroxidase-conjugated anti-mouse IgG for 1 h at room temperature and was imaged (ImageJ; Amersham Biosciences, Little Chalfont, UK) to quantify the signal.

Statistical analysis. All values are reported as means (SD), unless otherwise stated. P values <0.05 were considered statistically significant. Student's t-tests were used to assess differences between LPS and control groups. One-way ANOVA was used to test for differences in minimum oxygen-diffusion distance distributions and mRNA expression of HIF-1α, VEGF, and GLUT1 genes under different conditions. The Holm-Sidak test was used to test all multiple pair-wise comparisons between groups. Repeated-measures ANOVA was used to assess differences in protein and gene expression over time in isolated cardiomyocyte experiments. Linear regression was used to assess the correlation between E_{max} and gene expression. All statistical tests were performed by using SigmaStat 3.0 (Systat Software, Richmond, CA).

Table 1. *List of primers used for real-time RT-PCR*

Gene Name	Real-Time RT-PCR Primer, 5′ to 3′	
	Forward	Reverse
HIF-1α	TGCTTGGTGCTGATTTGTGAA	TATCGAGGCTGTGTCGACTGAG
VEGF	GCAATGATGAAGCCCTGGAG	GGTGAGGTTTGATCCGCATG
GLUT1	GGTGTGCAGCAGCCTGTGTA	GACGAACAGCGACACCACAGT
18s	CTTTGGTCGCTCGCTCCTC	CTGACCGGGTTGGTTTTGAT

HIF, hypoxia-inducible factor; GLUT, glucose transporter.

RESULTS

Effect of LPS on heart function. Five hours after administration of LPS, rat heart rate increased 21.4%(SD 2.7; $P < 0.05$) without significant changes in either left-ventricular preload (end-diastolic pressure or volume) or afterload (end-systolic pressure). The most striking effect of LPS on heart function was a 47% (SD 20; $P < 0.05$) decrease in left-ventricular contractility, as measured by E_{max} (Fig. 1, Table 2). There were no differences, however, in cardiac output, arterial oxygen saturation, hematocrit, or hemoglobin concentration between LPS and control rats. Both leukocyte and platelet counts decreased in LPS rats relative to control ($P < 0.05$), consistent with the onset of a systemic inflammatory response (Table 2). The survival rate was 75% in LPS-treated rats ($n = 32$) compared with 100% in controls ($n = 20$) and 100% in the LAD group ($n = 4$).

Myocardial microvascular geometry and tissue oxygenation. Whereas global oxygen-delivery parameters remained unchanged, changes in microvascular geometry indicated that microvascular heterogeneity had increased in the left ventricle relative to control. On the basis of confocal imaging of the myocardial microcirculation, we found the minimum oxygen-diffusion distance increased from 3.4 (SD 0.5) in control to 4.3 μm (SD 0.6) in LPS ($P < 0.05$, as shown in Fig. 2*C*, *inset*); moreover, minimum oxygen-diffusion distances >7 μm doubled from 10.7 (SD 4.4) to 22.4% (SD 6.6; $P < 0.05$; Fig. 2). Having found changes in microvascular heterogeneity that would affect the distribution of red blood cell and oxygen flow within the heart, and consequently tissue oxygenation, it was important to determine whether the heart became hypoxic during the onset of endotoxemia. Using a Po_2 probe inserted into the left ventricle, we found that myocardial tissue Po_2 decreased 47% (SD 17) in LPS-treated animals compared with control [from 9.6 (SD 4.1) to 4.8 mmHg (SD 2.2); $P < 0.05$; Fig. 2*E*], indicating that the left ventricle was hypoxic.

Gene-expression kinetics under hypoxic and inflammatory stimulation. Because LPS induced left-ventricular hypoxia at 5 h, we evaluated the effect of a similar degree of hypoxia (Po_2 = 5 mmHg) on hypoxia-inducible gene expression in isolated rat cardiomyocytes by determining the kinetics of HIF-1α protein stabilization and HIF-1α, VEGF, and GLUT1 gene expression (Fig. 3). HIF-1α protein and HIF-1α mRNA expression both increased transiently ($P < 0.05$) within the first 1–2 h, returning to baseline by 5 h. In contrast, VEGF mRNA increased slowly by twofold ($P < 0.05$), whereas GLUT1 mRNA increased rapidly by sixfold ($P < 0.05$) over the 5-h period. Because LPS increases the expression of TNF-α in cardiomyocytes (31), and because plasma levels of TNF-α increase following LPS administration (6), cardiomyocytes were also exposed to TNF-α under normoxic conditions (Fig. 3, *B* and *E*). Under normoxic conditions, TNF-α caused a similar, but delayed, transient HIF-1α protein and HIF-1α mRNA response relative to the hypoxic response (Fig. 3, *A* and *D*). And although there was no difference in the kinetics of

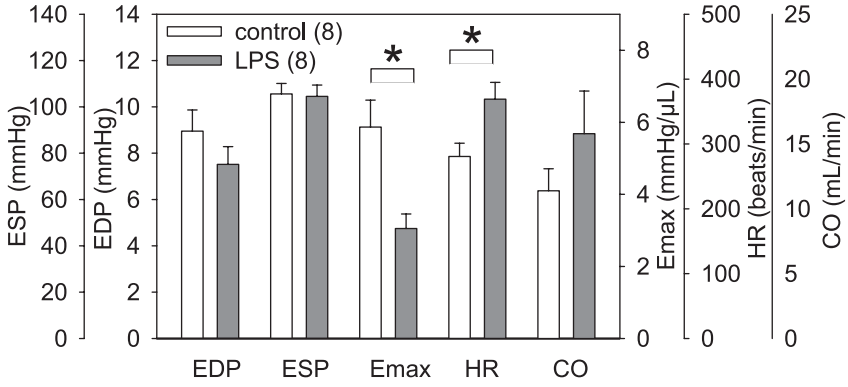

Fig. 1. Myocardial function 5 h after LPS administration. Myocardial functional parameters were determined by using a pressure-volume conductance catheter inserted into the left ventricle. EDP, end-diastolic pressure; ESP, end-systolic pressure; E_{max}, maximum elastance (a measure of left-ventricular contractility); HR, heart rate; CO, cardiac output. *$P < 0.05$.

VEGF gene expression between hypoxic and normoxic TNF-α conditions, because a similar twofold increase was found, GLUT1 gene expression was attenuated under normoxic TNF-α conditions relative to hypoxia (threefold compared with sixfold; $P < 0.05$). When cardiomyocytes were subjected to combined hypoxia and TNF-α stimulation (Fig. 3, *C* and *F*), the kinetics of HIF-1α protein stabilization and gene expression of HIF-1α, VEGF, and GLUT1 all resembled that of the response to hypoxia alone. Under hypoxic conditions, HIF-1α protein was stabilized to a greater degree than the HIF-1α gene was induced (Fig. 3*A*). In terms of gene expression, the hypoxia-inducible response was heterogeneous, because HIF-1α gene expression was the strongest early indicator of hypoxia, whereas GLUT1 gene expression was the strongest indicator of prolonged hypoxia.

Comparison of hypoxic gene expression under hypoxic and inflammatory conditions. Having associated increased microvascular heterogeneity with myocardial tissue hypoxia 5 h after LPS administration, and having assessed gene expression in isolated cardiomyocytes under hypoxic conditions, we asked whether hypoxia-induced gene expression was similarly spatially heterogeneous and related to areas of tissue inflammation in the rat heart 5 h after LPS administration. Using immunohistochemistry to identify regions of ICAM-1 protein expression, we found ICAM-1 to be heterogeneously overexpressed by fivefold ($P < 0.05$) in endotoxemic rat hearts (Fig. 4). In myocardial tissue regions with ICAM-1 overexpression, both HIF-1α and GLUT1 gene induction were higher ($P < 0.05$) than in non-ICAM-1 tissue background, whereas there was no difference in VEGF gene induction (Fig. 5). Comparing all treatment groups at the 5-h time point (Fig. 5), HIF-1α gene induction was greatest in ICAM-1 regions of endotoxemic hearts, VEGF gene induction was elevated to the same degree in all treatment groups, and GLUT1 gene induction was highly variable between groups. Compared with ICAM-1 regions of endotoxemic hearts, GLUT1 gene expression was increased relative to non-ICAM-1 background ($P < 0.05$), comparable with that in LAD control hearts but less than that observed in hypoxic cardiomyocytes ($P < 0.05$; Fig. 5).

Vector analysis of hypoxia gene expression. We used normalized gene expressions of HIF-1α, VEGF, and GLUT1 (relative to control) expressed as vectors to define a hypoxia-inducible gene expression "signature." We then calculated the fractional similarity between our experimental conditions as the inner product of these vectors. (This is the cosine of the angle between the expression vectors. If the two vectors line up exactly, the cosine is 1, whereas if one vector does not overlap at all with the other, the cosine is 0.) We found that gene expression of hypoxic cardiomyocytes was 96% similar to gene expression in heart tissue following LAD occlusion [P_{O_2} = 1.5 mmHg (SD 0.7)]. Thus this pattern defines a hypoxia-inducible gene-expression signature. The hypoxia-inducible gene signature found in the left ventricle of LPS hearts was 78% similar to the LAD condition, 42% similar to hypoxic cardiomyocytes, 83% similar to TNF-α-stimulated cardiomyocytes, and 75% similar to ICAM-1-expressing regions.

Correlation between heart contractility and gene expression. Of the three hypoxia-inducible target genes examined in this study (HIF-1α, VEGF, and GLUT1), only GLUT1 was found to have a significant correlation with left-ventricular contractility, as measured by E_{max}, 5 h after LPS administration (Fig. 6). Although both VEGF and HIF-1α expression showed trends toward a correlation with E_{max} ($P = 0.08$ and $P = 0.15$, respectively), no significant relationships were detected.

Table 2. *Heart function and systemic hemodynamic parameters*

Parameter	Control	LPS	Student's *t*-Test
Stroke volume, μl	42.8 (SD 21.2)	39.0 (SD 15.0)	NS
LVEDV, μl	189.3 (SD 19.8)	213.2 (SD 17.8)	NS
Systolic arterial pressure, mmHg	108.6 (SD 7.1)	105.0 (SD 7.5)	NS
Arterial oxygen saturation, %	94.9 (SD 0.9)	92.9 (SD 5.0)	NS
Hematocrit, %	43.1 (SD 2.0)	43.0 (SD 2.1)	NS
Hemoglobin, g/l	151.6 (SD 10.3)	148.6 (SD 7.5)	NS
White blood cell count, 10^9/l	7.3 (SD 2.8)	2.6 (SD 0.8)	$P < 0.05$
Platelet count, 10^9/l	1174 (SD 160)	540.3 (SD 200)	$P < 0.05$

Values are means (SD); n = 8/group. LVEDV, left ventricular end-diastolic volume; NS, nonsignificant difference.

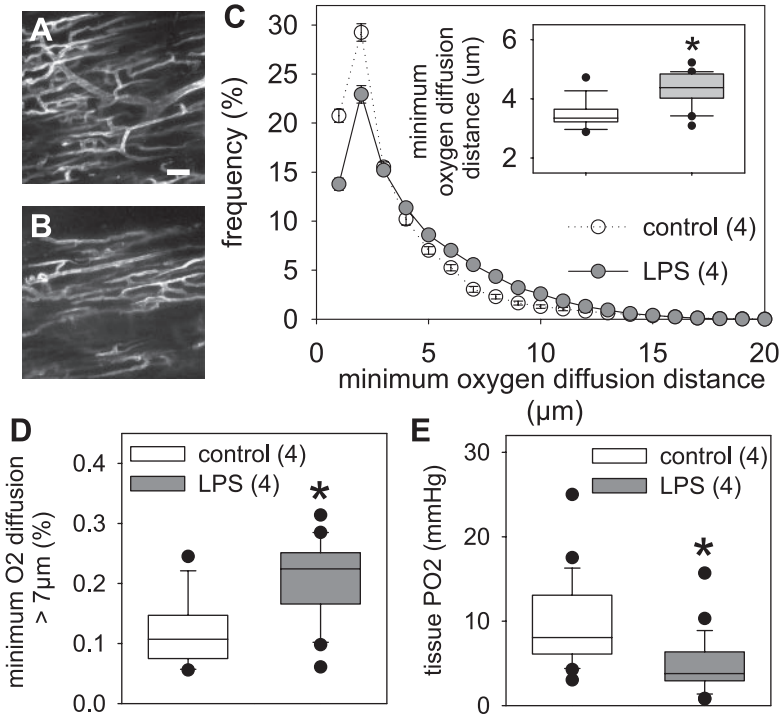

Fig. 2. Effect of LPS on myocardial microvascular minimum oxygen-diffusion distances and tissue oxygenation. Five hours after LPS administration, hearts were removed and endothelial cells were fluorescently labeled with $DiOC_{18}$ (excitation/emission = 484/501 nm). The left ventricle was imaged by confocal laser-scanning microscopy. *A* and *B*: representative top-down views of reconstructed 3-dimensional images. Myocardial microvascular geometry was quantified on the basis of shortest tissue voxel-to-capillary distance and was expressed as the frequency distribution of minimum oxygen-diffusion distances within the left ventricle (*C* and *C*, *inset*). The fraction of myocardium >7 μm from the nearest capillary is shown in *D*. Tissue oxygenation was determined by inserting a fluorescent P_{O_2} probe 1–2 mm into the surface of the left ventricle (*E*). *$P < 0.05$. Bar, 40 μm.

DISCUSSION

In this study, the key findings were that LPS increased oxygen-diffusion distances and decreased tissue oxygenation in the left ventricle while simultaneously increasing hypoxia-inducible HIF-1α, VEGF, and GLUT1 gene expression and decreasing left ventricle contractility. Gene induction was not homogeneous, but rather both HIF-1α and GLUT1 were overexpressed in heterogeneous regions of ICAM-1 expression, whereas VEGF was not. Five hours after administration of LPS, we found that GLUT1 gene expression correlated with left-ventricular contractility, suggesting that increased glucose metabolism may play a role in heart function during endotoxemia. The results also suggest that increased hypoxia-inducible gene expression, induced by both hypoxic and nonhypoxic signaling pathways, may be cardioprotective.

Myocardial microvascular heterogeneity and tissue oxygenation. Under normal hemodynamic conditions, cardiac output is such that global and local oxygen supply exceeds local oxygen demand. At the microregional level, the microcirculation regulates and distributes red blood cells and oxygen throughout the tissue to maintain tissue oxygen homeostasis (8). However, despite normal or enhanced cardiac output during sepsis, distribution and regulation of local tissue oxygen delivery are compromised by decreased functional capillary density (6, 7, 11, 17, 21, 26) and diminished conducted microvascular vasoconstriction (29). In our study, although LPS had no effect on global oxygen transport parameters, local myo-

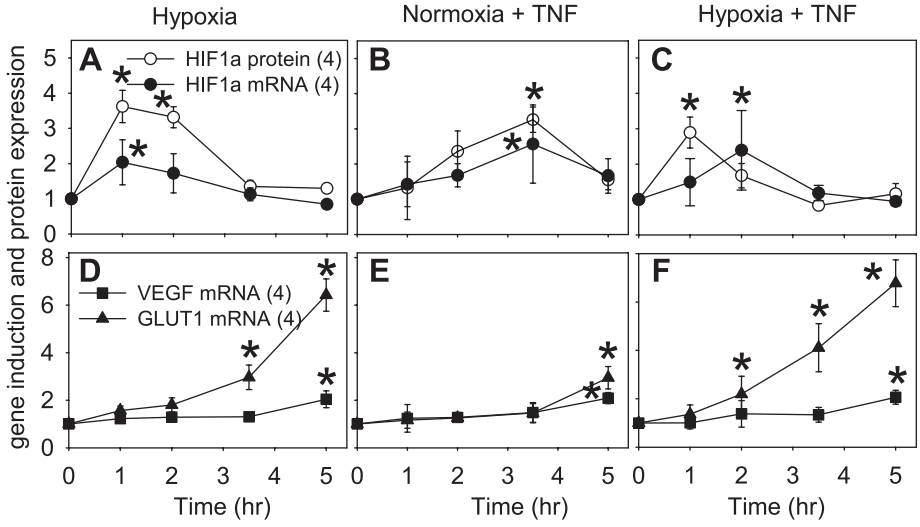

Fig. 3. Kinetics of hypoxia-inducible gene expression. Isolated rat cardiomyocytes were placed in a hypoxic chamber at P_{O_2} = 5 mmHg, and their medium was exchanged with medium equilibrated to chamber conditions. Cells were subjected to hypoxia (*A* and *D*), normoxia + TNF-α (*B* and *E*), and hypoxia + TNF-α (*C* and *F*) conditions. Hypoxia-inducible factor (HIF)-1α protein level (*A–C*) was determined by Western blot. Gene expression was quantified by using real-time RT-PCR. HIF-1α (*A–C*), VEGF (*D–F*), and glucose transporter (GLUT) 1 (*D–F*) gene expression were normalized to 18s gene expression and were plotted relative to *time 0*. *$P < 0.05$ relative to baseline.

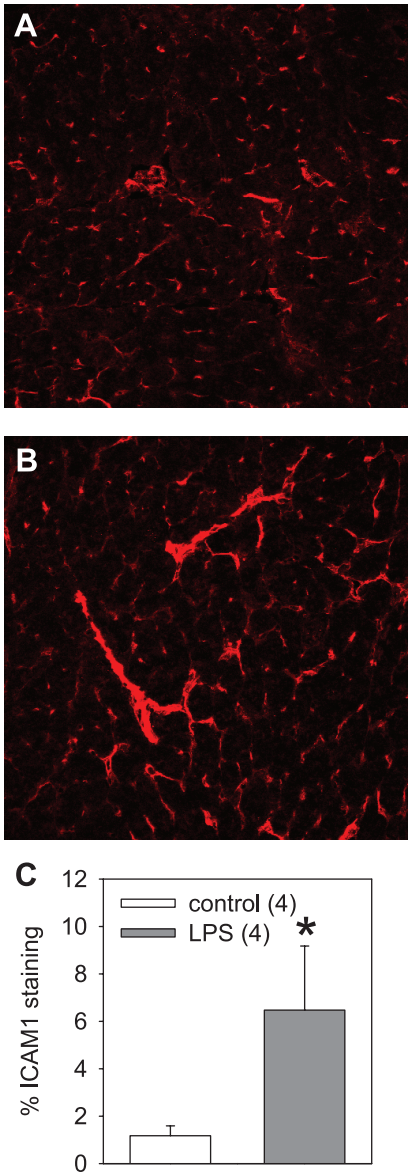

Fig. 4. Left ventricle ICAM-1 expression at 5 h. ICAM-1 expression in myocardial tissue was detected immunohistochemically. Confocal images of ICAM-1 staining heterogeneity are shown for control (*A*) and LPS-treated (*B*) rats. The degree of tissue expression (*C*) was quantified by establishing an image threshold value in control samples by using MATLAB [Otsu's method (30)] and then applying this value to LPS hearts. *$P < 0.05$.

cardial microvascular oxygen transport was disturbed. We found evidence of increased oxygen-diffusion distances within the left ventricle, consistent with findings that LPS decreases functional capillary density in the heart (6).

Loss of capillary density is mediated in part by leukocyte adhesion (6, 19) and reduced erythrocyte deformability (7). These events occur early in the onset of sepsis and cause physical plugging of individual capillaries in both skeletal and heart muscle tissue (6, 7, 17). No data yet exists that fully characterizes the nature of the microvascular injury in the in vivo septic heart. In septic skeletal muscle, however, in vivo studies have revealed a complex microvascular derangement that increases microvascular heterogeneity by altering microvascular geometry, flow distribution, and oxygen diffusion. This is manifested by loss of functional capillary density and increased oxygen-diffusion distances (consistent with our findings in the endotoxemic rat heart) (7, 11, 17, 26), as well as increased fast flow or shunting of red blood cell flow through some capillaries and reversal of red blood cell flow in others (8, 17) and, perhaps most importantly, an inability of the microcirculation to regulate capillary red blood cell flow (17) to match local oxygen supply with local oxygen demand.

Consistent with experimental findings, theoretical models and biosimulations (20, 21, 41) predict that increased microvascular heterogeneity will decrease tissue oxygen extraction in the heart (14, 16, 22) and will increase tissue hypoxia in skeletal muscle (2, 3, 21). In our study, we found the left ventricle of control rats to have a baseline tissue P_{O_2} of 9.6 mmHg (SD 1.0), consistent with myocardial P_{O_2} measurements made in mice by using electron paramagnetic resonance (EPR) spectroscopy (49) and in piglets by using phosphorescence (33). Five hours after LPS administration, tissue oxygenation decreased in the left ventricle, consistent with increased NADH levels in endotoxemic rat hearts (50). We found no differences in cardiac output, arterial oxygen saturation, or hemoglobin concentration, indicating that global oxygen delivery was unaffected by LPS. Because blood flow remains constant or increases in endotoxemic rat hearts (5, 27, 40), the myocardial tissue hypoxia observed in our study was not likely due to hypoperfusion; rather, decreased capillary density, increased microvascular heterogeneity, and mismatch of micro-

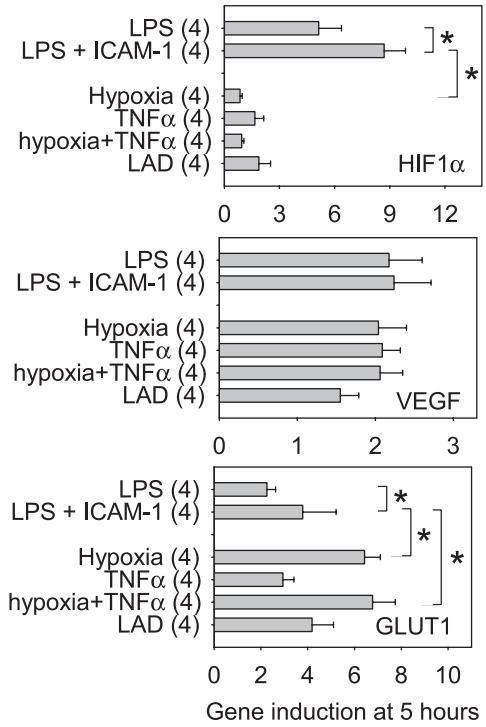

Fig. 5. Hypoxia-inducible gene induction at 5 h. HIF-1α, VEGF, and GLUT1 gene induction were determined by normalizing gene expression under different conditions to their respective control conditions. Gene expression itself was quantified by using real-time RT-PCR relative to 18s. LPS + ICAM-1 is gene expression in myocardial tissue sampled from regions with ICAM-1 expression. LPS is non-ICAM-1 background tissue. Hypoxia, TNF-α, and Hypoxia + TNF-α indicate gene expression in hypoxic and TNF-α-stimulated cardiomyocytes. LAD is a positive myocardial in vivo hypoxic control in left anterior descending coronary artery. *$P < 0.05$. (4), number of animal experiments.

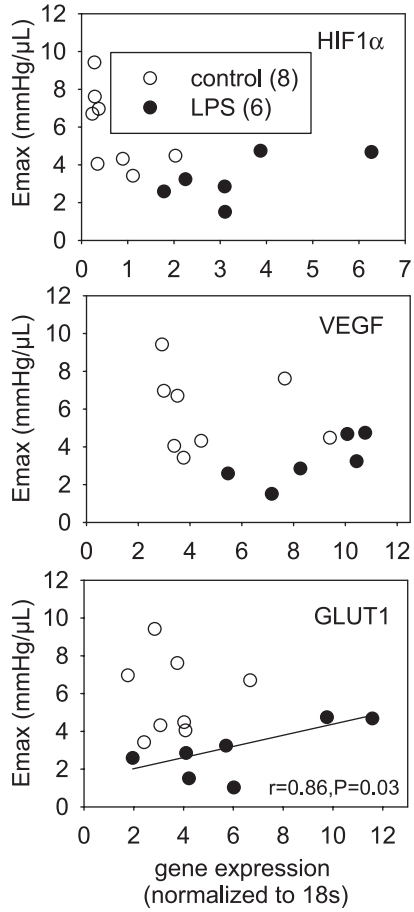

Fig. 6. Correlation between myocardial contractility and gene expression. Plots show the correlation between E_{max}, an independent measure of myocardial contractility, and hypoxia-inducible gene expression at 5 h. GLUT1 shows a positive correlation with heart function ($r = 0.86$, $P = 0.026$), suggesting that a shift to increased glucose or anaerobic metabolism during endotoxemia was beneficial for heart function. (6) and (8), number of animal experiments.

regional oxygen supply to increased oxygen demand (32) appear to be important factors.

Hypoxia-inducible gene expression in the endotoxemic heart. Having established that LPS induced myocardial hypoxia in the rat left ventricle 5 h after administration, we investigated whether this degree of hypoxia was sufficient to upregulate the hypoxia-inducible genes HIF-1α, VEGF, and GLUT1. In isolated rat cardiomyocytes, under hypoxic conditions similar to those observed in the endotoxemic rat heart, we found that both HIF-1α protein and HIF-1α mRNA were rapidly and transiently increased. This was consistent with the HIF-1α response in hypoxic macrophages (10), human monocytes (18), human HeLa cells (24), and rat liver (35), but contrary to findings in Hep 3B or HeLaS3 cells subjected to 0.5% oxygen for 4 h (45). In our study, a similar but delayed HIF-1α response was observed when normoxic cardiomyocytes were treated with TNF-α. This indicates that HIF-1α is transcriptionally regulated in rat cardiomyocytes via both hypoxic and nonhypoxic inflammatory signaling pathways. This is significant because LPS induces both increased myocardial TNF-α expression (31) and increased plasma TNF-α levels (6), as well as myocardial tissue hypoxia. In contrast to the synergistic effect between LPS and hypoxia on HIF-1α induction in human monocytes (18), we found no synergistic effect between TNF-α and hypoxia on HIF-1α gene expression in isolated cardiomyocytes. Five hours after LPS treatment, HIF-1α gene expression was increased in myocardial regions with ICAM-1 staining, indicating that the tissue inflammatory response was temporally and spatially associated with hypoxia-inducible gene expression during the onset of sepsis.

The "classical response" to hypoxia involves upregulation of the GLUT1 glucose transporter and glycolytic enzymes through a HIF-1-dependent mechanism (9), as well as translocation of GLUT4 and increased glucose uptake. Increased GLUT1 gene expression is also part of a coordinated response to preserve neonatal cardiomyocyte viability under conditions of metabolic inhibition (47) and may reflect a state of myocardial hibernation (28). In our study, we found the GLUT1 gene to be strongly induced in hypoxic rat cardiomyocytes. And although GLUT1 gene expression was less responsive to TNF-α, this nevertheless indicated that GLUT1 was transcriptionally regulated in cardiomyocytes via both hypoxic and nonhypoxic inflammatory signaling pathways. Similar to HIF-1α, GLUT1 was overexpressed in ICAM-1 regions of the endotoxemic left ventricle, again indicating that hypoxia-inducible gene expression was related to tissue inflammation. GLUT1 expression also correlated with left-ventricular contractility, suggesting that increased GLUT1 transport and enhanced glucose metabolism were beneficial to heart function during the onset of endotoxemia. However, because E_{max} is a multifactorial process, additional factors including upregulation of HIF-1α (although this study was underpowered to detect a correlation) and glycolytic enzymes (35) may also be involved in modulating heart function.

In addition to increasing glycolytic capacity, hypoxia also stimulates the growth of new blood vessels to enhance local oxygen delivery by upregulating VEGF (48). In our study, we found VEGF gene expression in hypoxic cardiomyocytes to be slowly upregulated and weaker than either HIF-1α or GLUT1 and to be similarly induced by both hypoxia and TNF-α. Consistent with HIF-1α and GLUT1, VEGF was transcriptionally regulated in cardiomyocytes via both hypoxic and nonhypoxic inflammatory signaling pathways. Contrary to HIF-1α and GLUT1, VEGF was not overexpressed in ICAM-1 regions in the left ventricle of LPS-treated rats, although it was overexpressed overall in the septic heart, indicative of a more diffuse VEGF response throughout the left ventricle. Because both VEGF and GLUT1 genes contain hypoxia-response elements in their respective promoter regions, we expected to find similar degrees of gene induction. The differences in degree, spatial, and temporal gene induction suggest that additional transcription factors besides HIF-1 (44, 46) were governing VEGF and GLUT1 gene expression during the onset of endotoxemia. Of note is that both heart function and sublingual microvascular perfusion density improve in patients who recover from sepsis (34). Whether the microcirculation clears or VEGF production mediates remodeling of myocardial capillary density, which in turn improves heart function, is unknown.

On the basis of vector analysis of target gene expression at 5 h, we found that the HIF-1α, VEGF, and GLUT1 hypoxia-inducible gene signature in the endotoxemic (LPS-treated) left ventricle most closely resembled both the positive in vivo hypoxic LAD control and the isolated cardiomyocytes treated with TNF-α. This was a somewhat unexpected result, given

that LPS induced hypoxia in the left ventricle. Nevertheless, it suggests that inflammatory mediators, including TNF-α, may be a factor in the initiation of hypoxia-inducible gene expression during the onset of sepsis, consistent with our findings in isolated cardiomyocytes. Increased HIF-1α and GLUT1 gene induction in ICAM-1 regions also suggests that local inflammation, possibly mediated by leukocyte plugging, is temporally and spatially associated with hypoxia-inducible gene expression and microregional hypoxia.

Study limitations. It is possible that the ex vivo microvascular labeling procedure underestimated the degree of stopped flow in the heart. Although we found a significant increase in the minimum oxygen-diffusion distance in LPS hearts, consistent with in vivo loss of functional capillary density in skeletal muscle (17, 26), the in vivo minimum oxygen-diffusion distance may have been greater. Due to the relatively large P_{O_2} probe diameter, tissue-oxygenation measurements include oxygen sources from local microvessels as well as tissue, and thus local tissue P_{O_2} may be lower than reported.

Conclusions. The pattern of high HIF-1α and low GLUT1 gene induction in the left ventricle 5 h after LPS administration is the inverse situation of the low HIF-1α and high GLUT1 gene induction found in isolated hypoxic cardiomyocytes after 5 h. A possible explanation for this discrepancy is that hypoxia was delayed by several hours following the administration of LPS. In the context of a progressive septic microvascular injury, it is conceivable that early inflammatory mediators initiate hypoxia-inducible gene expression in the heart, whereas later tissue hypoxia, resulting from increased microvascular heterogeneity, either sustains or expands the response. The subsequent adaptive cardiomyocyte response to local inflammatory and hypoxic microregional conditions may facilitate preservation and eventual recovery of organ function, provided the host is not overwhelmed by the septic injury.

ACKNOWLEDGMENTS

We acknowledge the help of Amrit Samra with tissue sectioning, Shelley Dai with real time RT-PCR, Yingjin Wang with animal experiments, and Dr. Elaine Humphrey for discussions regarding confocal microscopy.

GRANTS

This study was supported by an operating grant from the Canadian Institutes of Health Research. R. M. Bateman is a Heart and Stroke Foundation, Michael Smith Foundation for Health Research, and Canadian Institutes of Health Research/Heart and Stroke Foundation of Canada IMPACT Strategic Training Postdoctoral Fellow. K. R. Walley is a Michael Smith Foundation for Health Research Distinguished Scholar.

REFERENCES

1. **Angus DC, Linde-Zwirble WT, Lidicker J, Clermont G, Carcillo J, Pinsky MR.** Epidemiology of severe sepsis in the United States: analysis of incidence, outcome, and associated costs of care. *Crit Care Med* 29: 1303–1310, 2001.
2. **Anning PB, Sair M, Winlove CP, Evans TW.** Abnormal tissue oxygenation and cardiovascular changes in endotoxemia. *Am J Respir Crit Care Med* 159: 1710–1715, 1999.
3. **Astiz M, Rackow EC, Weil MH, Schumer W.** Early impairment of oxidative metabolism and energy production in severe sepsis. *Circ Shock* 26: 311–320, 1988.
4. **Avontuur JA, Bruining HA, Ince C.** Inhibition of nitric oxide synthesis causes myocardial ischemia in endotoxemic rats. *Circ Res* 76: 418–425, 1995.
5. **Avontuur JA, Bruining HA, Ince C.** Nitric oxide causes dysfunction of coronary autoregulation in endotoxemic rats. *Cardiovasc Res* 35: 368–376, 1997.
6. **Barroso-Aranda J, Schmid-Schonbein GW, Zweifach BW, Mathison JC.** Polymorphonuclear neutrophil contribution to induced tolerance to bacterial lipopolysaccharide. *Circ Res* 69: 1196–1206, 1991.
7. **Bateman RM, Jagger JE, Sharpe MD, Ellsworth ML, Mehta S, Ellis CG.** Erythrocyte deformability is a nitric oxide-mediated factor in decreased capillary density during sepsis. *Am J Physiol Heart Circ Physiol* 280: H2848–H2856, 2001.
8. **Bateman RM, Sharpe MD, Ellis CG.** Bench-to-bedside review: microvascular dysfunction in sepsis—hemodynamics, oxygen transport, and nitric oxide. *Crit Care* 7: 359–373, 2003.
9. **Behrooz A, Ismail-Beigi F.** Dual control of glut1 glucose transporter gene expression by hypoxia and by inhibition of oxidative phosphorylation. *J Biol Chem* 272: 5555–5562, 1997.
10. **Blouin CC, Page EL, Soucy GM, Richard DE.** Hypoxic gene activation by lipopolysaccharide in macrophages: implication of hypoxia-inducible factor 1alpha. *Blood* 103: 1124–1130, 2004.
11. **Boczkowski J, Vicaut E, Aubier M.** In vivo effects of *Escherichia coli* endotoxemia on diaphragmatic microcirculation in rats. *J Appl Physiol* 72: 2219–2224, 1992.
12. **Bosan S, Kareco T, Ruehlmann D, Chen KY, Walley KR.** Three-dimensional capillary geometry in gut tissue. *Microsc Res Tech* 61: 428–437, 2003.
13. **Braun RD, Lanzen JL, Snyder SA, Dewhirst MW.** Comparison of tumor and normal tissue oxygen tension measurements using OxyLite or microelectrodes in rodents. *Am J Physiol Heart Circ Physiol* 280: H2533–H2544, 2001.
14. **Cunnion RE, Schaer GL, Parker MM, Natanson C, Parrillo JE.** The coronary circulation in human septic shock. *Circulation* 73: 637–644, 1986.
15. **Davani EY, Dorscheid DR, Lee CH, van Breemen C, Walley KR.** Novel regulatory mechanism of cardiomyocyte contractility involving ICAM-1 and the cytoskeleton. *Am J Physiol Heart Circ Physiol* 287: H1013–H1022, 2004.
16. **Dhainaut JF, Huyghebaert MF, Monsallier JF, Lefevre G, Dall'Ava-Santucci J, Brunet F, Villemant D, Carli A, Raichvarg D.** Coronary hemodynamics and myocardial metabolism of lactate, free fatty acids, glucose, and ketones in patients with septic shock. *Circulation* 75: 533–541, 1987.
17. **Ellis CG, Bateman RM, Sharpe MD, Sibbald WJ, Gill R.** Effect of a maldistribution of microvascular blood flow on capillary O_2 extraction in sepsis. *Am J Physiol Heart Circ Physiol* 282: H156–H164, 2002.
18. **Frede S, Stockmann C, Freitag P, Fandrey J.** Bacterial lipopolysaccharide induces HIF-1 activation in human monocytes via p44/42 MAPK and NF-kappaB. *Biochem J* 396: 517–527, 2006.
19. **Goddard CM, Allard MF, Hogg JC, Herbertson MJ, Walley KR.** Prolonged leukocyte transit time in coronary microcirculation of endotoxemic pigs. *Am J Physiol Heart Circ Physiol* 269: H1389–H1397, 1995.
20. **Goldman D, Bateman RM, Ellis CG.** Effect of decreased O_2 supply on skeletal muscle oxygenation and O_2 consumption during sepsis: role of heterogeneous capillary spacing and blood flow. *Am J Physiol Heart Circ Physiol* 290: H2277–H2285, 2006.
21. **Goldman D, Bateman RM, Ellis CG.** Effect of sepsis on skeletal muscle oxygen consumption and tissue oxygenation: interpreting capillary oxygen transport data using a mathematical model. *Am J Physiol Heart Circ Physiol* 287: H2535–H2544, 2004.
22. **Herbertson MJ, Werner HA, Russell JA, Iversen K, Walley KR.** Myocardial oxygen extraction ratio is decreased during endotoxemia in pigs. *J Appl Physiol* 79: 479–486, 1995.
23. **Hotchkiss RS, Rust RS, Dence CS, Wasserman TH, Song SK, Hwang DR, Karl IE, Welch MJ.** Evaluation of the role of cellular hypoxia in sepsis by the hypoxic marker [^{18}F]fluoromisonidazole. *Am J Physiol Regul Integr Comp Physiol* 261: R965–R972, 1991.
24. **Jiang BH, Semenza GL, Bauer C, Marti HH.** Hypoxia-inducible factor 1 levels vary exponentially over a physiologically relevant range of O_2 tension. *Am J Physiol Cell Physiol* 271: C1172–C1180, 1996.
25. **Jurgensen JS, Rosenberger C, Wiesener MS, Warnecke C, Horstrup JH, Grafe M, Philipp S, Griethe W, Maxwell PH, Frei U, Bachmann S, Willenbrock R, Eckardt KU.** Persistent induction of HIF-1alpha and -2alpha in cardiomyocytes and stromal cells of ischemic myocardium. *FASEB J* 18: 1415–1417, 2004.
26. **Lam C, Tyml K, Martin C, Sibbald W.** Microvascular perfusion is impaired in a rat model of normotensive sepsis. *J Clin Invest* 94: 2077–2083, 1994.

27. **Lang CH, Bagby GJ, Ferguson JL, Spitzer JJ.** Cardiac output and redistribution of organ blood flow in hypermetabolic sepsis. *Am J Physiol Regul Integr Comp Physiol* 246: R331–R337, 1984.
28. **Levy RJ, Piel DA, Acton PD, Zhou R, Ferrari VA, Karp JS, Deutschman CS.** Evidence of myocardial hibernation in the septic heart. *Crit Care Med* 33: 2752–2756, 2005.
29. **McKinnon RL, Lidington D, Bolon M, Ouellette Y, Kidder GM, Tyml K.** Reduced arteriolar conducted vasoconstriction in septic mouse cremaster muscle is mediated by nNOS-derived NO. *Cardiovasc Res* 69: 236–244, 2006.
30. **Otsu N.** A threshold selection method from gray-level histograms. *IEEE Trans Sys Man Cyber* 9: 62–66, 1979.
31. **Peng T, Lu X, Lei M, Moe GW, Feng Q.** Inhibition of p38 MAPK decreases myocardial TNF-alpha expression and improves myocardial function and survival in endotoxemia. *Cardiovasc Res* 59: 893–900, 2003.
32. **Rumsey WL, Kilpatrick L, Wilson DF, Erecinska M.** Myocardial metabolism and coronary flow: effects of endotoxemia. *Am J Physiol Heart Circ Physiol* 255: H1295–H1304, 1988.
33. **Rumsey WL, Pawlowski M, Lejavardi N, Wilson DF.** Oxygen pressure distribution in the heart in vivo and evaluation of the ischemic "border zone". *Am J Physiol Heart Circ Physiol* 266: H1676–H1680, 1994.
34. **Sakr Y, Dubois MJ, De Backer D, Creteur J, Vincent JL.** Persistent microcirculatory alterations are associated with organ failure and death in patients with septic shock. *Crit Care Med* 32: 1825–1831, 2004.
35. **Scharte M, Han X, Uchiyama T, Tawadrous Z, Delude RL, Fink MP.** LPS increases hepatic HIF-1alpha protein and expression of the HIF-1-dependent gene aldolase A in rats. *J Surg Res* 135: 262–267, 2006.
36. **Semenza GL.** HIF-1, O_2, and the 3 PHDs: how animal cells signal hypoxia to the nucleus. *Cell* 107: 1–3, 2001.
37. **Semenza GL, Agani F, Iyer N, Kotch L, Laughner E, Leung S, Yu A.** Regulation of cardiovascular development and physiology by hypoxia-inducible factor 1. *Ann NY Acad Sci* 874: 262–268, 1999.
38. **Suga H.** Cardiac energetics: from E(max) to pressure-volume area. *Clin Exp Pharmacol Physiol* 30: 580–585, 2003.
39. **Sutter CH, Laughner E, Semenza GL.** Hypoxia-inducible factor 1alpha protein expression is controlled by oxygen-regulated ubiquitination that is disrupted by deletions and missense mutations. *Proc Natl Acad Sci USA* 97: 4748–4753, 2000.
40. **van Lambalgen AA, van Kraats AA, Mulder MF, van den Bos GC, Teerlink T, Thijs LG.** Organ blood flow and distribution of cardiac output in dopexamine- or dobutamine-treated endotoxemic rats. *J Crit Care* 8: 117–127, 1993.
41. **Walley KR.** Heterogeneity of oxygen delivery impairs oxygen extraction by peripheral tissues: theory. *J Appl Physiol* 81: 885–894, 1996.
42. **Walley KR, Becker CJ, Hogan RA, Teplinsky K, Wood LD.** Progressive hypoxemia limits left ventricular oxygen consumption and contractility. *Circ Res* 63: 849–859, 1988.
43. **Wang GL, Jiang BH, Rue EA, Semenza GL.** Hypoxia-inducible factor 1 is a basic-helix-loop-helix-PAS heterodimer regulated by cellular O_2 tension. *Proc Natl Acad Sci USA* 92: 5510–5514, 1995.
44. **Wang GL, Jiang BH, Semenza GL.** Effect of altered redox states on expression and DNA-binding activity of hypoxia-inducible factor 1. *Biochem Biophys Res Commun* 212: 550–556, 1995.
45. **Wenger RH, Kvietikova I, Rolfs A, Gassmann M, Marti HH.** Hypoxia-inducible factor-1 alpha is regulated at the post-mRNA level. *Kidney Int* 51: 560–563, 1997.
46. **Wenger RH, Stiehl DP, Camenisch G.** Integration of oxygen signaling at the consensus HRE. *Sci STKE* 2005: re12, 2005.
47. **Wright G, Higgin JJ, Raines RT, Steenbergen C, Murphy E.** Activation of the prolyl hydroxylase oxygen-sensor results in induction of GLUT1, heme oxygenase-1, and nitric-oxide synthase proteins and confers protection from metabolic inhibition to cardiomyocytes. *J Biol Chem* 278: 20235–20239, 2003.
48. **Yamakawa M, Liu LX, Date T, Belanger AJ, Vincent KA, Akita GY, Kuriyama T, Cheng SH, Gregory RJ, Jiang C.** Hypoxia-inducible factor-1 mediates activation of cultured vascular endothelial cells by inducing multiple angiogenic factors. *Circ Res* 93: 664–673, 2003.
49. **Zhao X, He G, Chen YR, Pandian RP, Kuppusamy P, Zweier JL.** Endothelium-derived nitric oxide regulates postischemic myocardial oxygenation and oxygen consumption by modulation of mitochondrial electron transport. *Circulation* 111: 2966–2972, 2005.
50. **Zuurbier CJ, van Iterson M, Ince C.** Functional heterogeneity of oxygen supply-consumption ratio in the heart. *Cardiovasc Res* 44: 488–497, 1999.